Acta Biochim Biophys Sin, 2018, 50(5), 491–498
doi: 10.1093/abbs/gmy024
Advance Access Publication Date: 12 March 2018
Original Article

Original Article

Anti-fibrotic role and mechanism of *Periplaneta americana* extracts in CCl_4-induced hepatic fibrosis in rats

Dingchun Li[1], Wu Li[1,*], Yihui Chen[1], Lihui Liu[1], Dehong Ma[2], Hongtu Wang[1], Lu Zhang[1], Shenjun Zhao[1], and Qin Peng[1]

[1]Department of Infectious Disease, The First Affiliated Hospital of Kunming Medical University, Kunming 650000, China, and [2]Department of Infectious Disease, Xishuangbanna Dai National Minority Autonomous Prefecture People's Hospital, Xishuangbanna Dai National Minority Autonomous Region, Jinghong 666100, China

*Correspondence address. Tel/Fax: +86-871-65324888; E-mail: liwukm@126.com

Received 9 August 2017; Editorial Decision 27 December 2017

Abstract

Hepatic fibrosis is resulted from sustained wound-healing responses to various harmful stimuli, including viral infection, drug toxicity, alcohol, and autoimmune hepatopathy, and it has recently attracted the attention of an increasing number of researchers and clinical workers. The aims of this study were to examine the anti-fibrotic effects of extracts of *Periplaneta americana* (EPA) on CCl_4-induced hepatic fibrosis in rats, to preliminary determine the anti-fibrotic efficacy of EPA, and to identify a potential and effective therapeutic agent to attenuate hepatic fibrosis. In this study, we routinely detected liver functional indices, such as alanine aminotransferase (ALT), aspartate transaminase (AST), and albumin (Alb). We also measured hepatic fibrosis-related serum markers, including hyaluronic acid (HA), laminin (LN), type III procollagen (PC III), and type IV collagen (IV-C) via radioimmunoassay. Moreover, we examined histological activity and fibrosis stage via light microscopy after hematoxylin and eosin and Masson staining. Furthermore, we detected the expressions of nuclear factor-kappa B (NF-κB), alpha-smooth muscle actin (α-SMA), transforming growth factor-β1 (TGF-β1), and tissue inhibitor of metalloprotease-1 (TIMP-1) in rat liver tissues by immunohistochemical staining. We found that EPA, whose main components are viscous sugar amino acids, can reduce the levels hepatic fibrosis-related factors, including HA, LN, PC III, and IV-C, improve liver function, attenuate, or reverse pathological damage associated with hepatic fibrosis, and thus inhibit the progression of hepatic fibrosis. The mechanism of EPA action may be related to the inhibition of TGF-β1, NF-κB, and α-SMA expressions and the reduction of TIMP-1 levels in the liver to reduce the accumulation of extracellular matrix (ECM) components, thereby blocking the relevant signaling pathways and preventing inflammatory responses to attenuate or reverse hepatic fibrosis. EPA may thus be used as a potentially effective therapeutic agent for the treatment of hepatic fibrosis.

Key words: hepatic fibrosis, extracts of *Periplaneta americana*, TGF-β1, TIMP-1, NF-κB, α-SMA

Introduction

Hepatic fibrosis is resulted from sustained wound-healing responses to various harmful stimuli, including viral infection, drug toxicity, alcohol, and autoimmune hepatopathy [1]. It is an important pathologic hallmark of chronic liver diseases, a key event in the development of liver cirrhosis and a leading cause of end-stage hepatocellular carcinoma [2]. With advancements in the research of hepatic fibrosis, there have been immense improvements in the understanding of hepatic

fibrosis that leads to the reversal of compensatory cirrhosis as well as late-stage liver cirrhosis [3]. Extracts of *Periplaneta americana* (EPA) contain a variety of compounds that can kill bacteria, fungi, viruses, protozoa, and even cancer cells. The main components of EPA are viscous sugar amino acids. Studies have shown that EPA can exert protective effects against liver injury, inhibit the replication of hepatitis B virus in ducklings, and normalize liver enzymes to attenuate hepatocyte damage caused by carbon tetrachloride (CCl_4) [4,5]. Our previous studies have shown that EPA can exert a beneficial effect on mice with CCl_4-induced hepatic fibrosis [6,7].

In this study, to determine the anti-fibrotic effects of EPA, we used a CCl_4-induced rat hepatic fibrosis model to investigate the effects and anti-fibrotic efficacy of EPA on hepatic fibrosis.

Materials and Methods

Animal model and experimental design

Male Sprague Dawley rats (from 5- to 6-week-old and weighing 120–150 g) were obtained from the Laboratory Animal Center of Kunming Medical University. The animals had free access to water and food and were allowed to acclimatize to the environment for 1 week before experiments. All animals used in the study were housed under the same conditions in cages that were regularly cleaned and disinfected. Animals were treated according to the Animal Experiment Protocol: SCXK (Yunnan) 2011-0004.

Seventy rats were randomly divided into seven groups with 10 rats in each group, namely, the normal control group, the model group, the EPA high-dose group, the EPA medium-dose group, the EPA low-dose group, the notoginseng salvia miltiorrhiza group, and the colchicine positive control group. In all groups except for the normal control group, the CCl_4-induced hepatic fibrosis model was established by intraperitoneal injections of 0.05 ml/10 g of CCl_4 in olive oil twice a week for 7 weeks. The normal control group was intraperitoneally injected with an equal amount of olive oil. During the early stages of establishment of the hepatic fibrosis model, the EPA groups and the notoginseng salvia miltiorrhiza group were gavaged daily with 20 ml/kg body weight of the corresponding compounds, the colchicine group was gavaged daily with 10 ml/kg body weight of colchicine, and the normal control group and the model group were given 20 ml/kg body weight of physiological saline in the same manner. During the experiment, the activity, mental state, coat appearance, response to external stimuli, appetite, weight gain, and other general conditions of the rats were routinely monitored. At the end of the seventh week, after the last gavage, all rats were anesthetized by ether inhalation. Then, blood samples were collected from the rat abdominal aorta with a syringe and transferred it into centrifuge tubes containing an anticoagulant. The collected blood was used to test the levels of liver functional indices and hepatic fibrosis-related markers. Subsequently, the rats were euthanized, and liver specimens were collected for histopathological and immunohistochemical analyses.

Experimental materials

EPA was purchased from Kunming Sainuo Pharmacy Co., Ltd (serial number: 03122001; Kunming, China) and made into 2.5%, 1.25%, and 0.5% suspensions in distilled water. Notoginseng salvia miltiorrhiza was obtained from the First Affiliated Hospital of Kunming Medical University (serial number: 20120513); each piece weighed 0.33 g (containing 0.26 g equivalent of crude drugs). The appropriate amount of the pieces was ground in a mortar, mixed with distilled water to the required concentration, and stored in the refrigerator until use. Colchicine was purchased from Yunnan Plant Pharmaceutical Co. (Kunming, China), dissolved (1 mg/100 ml) in distilled water, and stored in the refrigerator until use. Purified CCl_4 (product number: 1017499) and purified olive oil (product number: GC1270) were obtained from Kunming Ze Hao Technology Co. (Kunming, China). CCl_4 was diluted to 20% (v/v) with olive oil before use. Radioimmunoassay kits for the detection of hyaluronic acid (HA), laminin (LN), type III procollagen (PC III), and type IV collagen (IV-C) were obtained from Beijing North Biotechnology Research Institute (Beijing, China). Immunohistochemistry kits for the detection of transforming growth factor-beta1 (TGF-β1), tissue inhibitor of metalloproteases-1 (TIMP-1), alpha-smooth muscle actin (α-SMA), and nuclear factor-kappa B (NF-κB) were obtained from Santa Cruz Biotech (Santa Cruz, USA), and the Masson kit was purchased from Fuzhou New Biotechnology Development Co. (Fuzhou, China).

Biochemical analysis

The levels of ALT, AST, and Alb in rat sera were determined using an automatic biochemical analyzer (Cobas C701; Roche Biotechnology, Basel, Switzerland). The serum levels of HA, LN, PC, and IV-C were detected by radioimmunoassay using the corresponding kits.

Histopathological examination

Liver tissues were fixed in formalin, embedded in paraffin, and sectioned to a thickness of 5 μm. Hematoxylin and eosin (H&E) staining was used to examine the changes in liver pathology. Collagen deposition in the liver was evaluated by Masson staining. Histological changes in the liver, collagen fiber hyperplasia, histological activity, and stage of fibrosis were evaluated under a light microscope. Hepatic fibrosis was graded based on the internationally used Metavir scoring system.

Immunohistochemical staining

Immunohistochemical staining was conducted according to the instruction manual provided with the kit. Deposition of brown particles in the portal area, the surrounding central vein, cytoplasm or 2 interstitial structures was considered positive staining. The staining intensity and the extent of staining for α-SMA, NF-κB, TGF-β1, and TIMP-1 were evaluated by light microscopy according to the recommendations provided with the kits. The average stained area for each of the above hepatic fibrosis-related protein markers was determined, and finally it is presented as a percentage.

Statistical analysis

All data were presented as the mean ± SD. Statistical analyses were performed with SPSS 17.0 software (Chicago, USA). Rank data were analyzed with the rank sum test. Student's *t*-test was used for comparison between two groups, and $P < 0.05$ was considered as statistically significant.

Results

General health of the rats

The overall health of the rats was good, with the normal control group having a higher weight than the model group before euthanasia. At the end of the experiment, rats in the model group showed reduced activity and appetite, yellow urine, poor nutrition, mental fatigue, rough and dull fur, lifeless eyes, and symptoms of chronic

diarrhea. One rat each died in the model group and in the EPA high-dose group, while the remaining rats survived to the end of the experiment.

Effect of EPA on CCl_4-induced hepatic fibrosis in rats

As shown in **Table 1**, the serum levels of ALT and AST were much higher in the model group than those in the normal group, EPA, notoginseng salvia miltiorrhiza and colchicine groups, respectively. The serum levels of Alb were much lower in the model group than those in the normal, EPA, notoginseng salvia miltiorrhiza, and colchicine groups. Although EPA, notoginseng salvia miltiorrhiza, and colchicine treatment clearly improved all of the above parameters compared with those in the model group, the improvements in ALT and AST levels were much better with EPA than with notoginseng salvia miltiorrhiza or colchicine ($P < 0.01$). However, there was no significant difference in the serum level of Alb in liver tissues between the EPA group and notoginseng salvia miltiorrhiza group or colchicine group ($P > 0.05$).

As shown in **Table 2**, HA, LN, PC III, and IV-C levels in rat sera were significantly decreased in all EPA groups as well as in the notoginseng salvia miltiorrhiza and colchicine groups. Except IV-C levels, the levels of the other indicators were significantly lower in all EPA groups than those in the notoginseng salvia miltiorrhiza and colchicine groups ($P < 0.05$).

Effect of EPA on the anatomical and histopathological appearance of liver samples

The rat livers in the model group appeared swollen, rough in texture, stiff, and dark in color, with many small nodules on the surface. However, the livers were ruddier in color and the edges were more regular in the normal, EPA, notoginseng salvia miltiorrhiza, and colchicine groups than those in the model group. At the end of the experiment, based on Masson staining (**Fig. 1**) and H&E staining (**Fig. 2**), liver tissue samples from rats in the normal group displayed normal lobular architecture with central veins, uniform cells, and neat rows of hepatic cords without degeneration. There was no evidence of fibrous tissue hyperplasia or pseudolobule, and liver cell necrosis or collagen fibers were occasionally observed in these liver tissue sections.

However, in contrast to those from the normal group, liver tissue sections from the model group displayed a markedly high number of inflammatory cell infiltrates, pronounced adipose degeneration of hepatocytes, extensive necrosis of hepatocytes around the lobule, and increased deposition of collagen fibers in hepatic lobules, all of which disturbed the lobular architecture and led to the formation of a pseudolobule that separated the lobules.

In contrast, histopathological examination of rat liver sections indicated that compared with those in the model group, adipose degeneration and necrosis of hepatocytes were markedly ameliorated, and migration and infiltration of inflammatory cells were reduced in the EPA, notoginseng salvia miltiorrhiza, and colchicine groups. In addition, there were more collagen fibers in the model group than those in the EPA, notoginseng salvia miltiorrhiza, and colchicine groups (**Figs. 1** and **2**).

All these results showed that compared with those in the model group, adipose degeneration and necrosis of hepatocytes were markedly ameliorated, migration and infiltration of inflammatory cells were reduced, and there were less collagen fibers in the EPA, notoginseng salvia miltiorrhiza, and colchicine groups.

Table 1. Serum levels of alanine ALT, AST, and Alb in the various groups

Groups	*n*	ALT (U/l)	AST (U/l)	Alb (g/l)
Normal	10	31.27 ± 2.11	39.42 ± 3.59	45.19 ± 3.62
Model	9	810.20 ± 54.60^{a}	144.92 ± 8.51^{a}	24.84 ± 2.20^{a}
EPA high dose	9	137.44 ± 13.47^{b}	72.90 ± 4.52^{b}	36.46 ± 2.63^{b}
EPA medium dose	10	152.91 ± 15.32^{b}	77.81 ± 6.60^{b}	36.21 ± 2.67^{b}
EPA low dose	9	210.27 ± 20.11^{b}	89.12 ± 7.98^{b}	35.98 ± 3.01^{b}
Drug 1	10	$264.29 \pm 34.72^{b,c}$	$97.68 \pm 5.40^{b,c}$	37.23 ± 2.30^{b}
Drug 2	10	$270.56 \pm 30.62^{b,c}$	$110.55 \pm 8.00^{b,c}$	36.18 ± 3.40^{b}

Data are presented as the mean ± SD.

ALT, alanine aminotransferase; AST, aspartate transaminase; Alb, albumin.

EPA, extracts of *P. americana*; Drug 1, notoginseng salvia miltiorrhiza; Drug 2, colchicine.

$^{a}P < 0.01$ compared with the normal group; $^{b}P < 0.01$ compared with the model group; and $^{c}P < 0.01$ compared with each EPA group.

Table 2. Serum levels of HA, LN, PC III, and IV-C in the various groups

Groups	*n*	HA (μg/l)	LN (μg/l)	PC III (μg/l)	IV-C (μg/l)
Normal	10	95.10 ± 19.83	55.35 ± 12.15	6.19 ± 1.74	30.73 ± 2.28
Model	9	456.80 ± 175.32^{a}	214.83 ± 35.76^{a}	29.40 ± 7.06^{a}	82.09 ± 7.97^{a}
EPA high dose	9	143.41 ± 28.93^{a}	94.24 ± 22.58^{b}	13.16 ± 2.16^{b}	56.95 ± 2.61^{b}
EPA medium dose	10	162.28 ± 14.18^{b}	118.71 ± 17.36^{b}	17.64 ± 2.09^{b}	60.61 ± 5.88^{b}
EPA low dose	10	210.74 ± 35.22^{b}	130.11 ± 18.32^{b}	21.54 ± 1.13^{b}	71.15 ± 4.76^{b}
Drug 1	10	$235.72 \pm 33.91^{b,c}$	$136.40 \pm 15.88^{b,c}$	$23.62 \pm 2.67^{b,c}$	71.73 ± 8.11^{b}
Drug 2	10	$242.87 \pm 38.75^{b,c}$	$137.63 \pm 11.19^{b,c}$	$24.55 \pm 2.84^{b,c}$	$63.49 \pm 4.62^{b,c}$

Data are presented as the mean ± SD.

HA, hyaluronic acid; LN, laminin; PC III, type III procollagen; IV-C, type IV collagen.

Drug 1, notoginseng salvia miltiorrhiza; Drug 2, colchicine.

$^{a}P < 0.01$ compared with the normal group; $^{b}P < 0.05$ compared with the model group; and $^{c}P < 0.05$ compared with each EPA group.

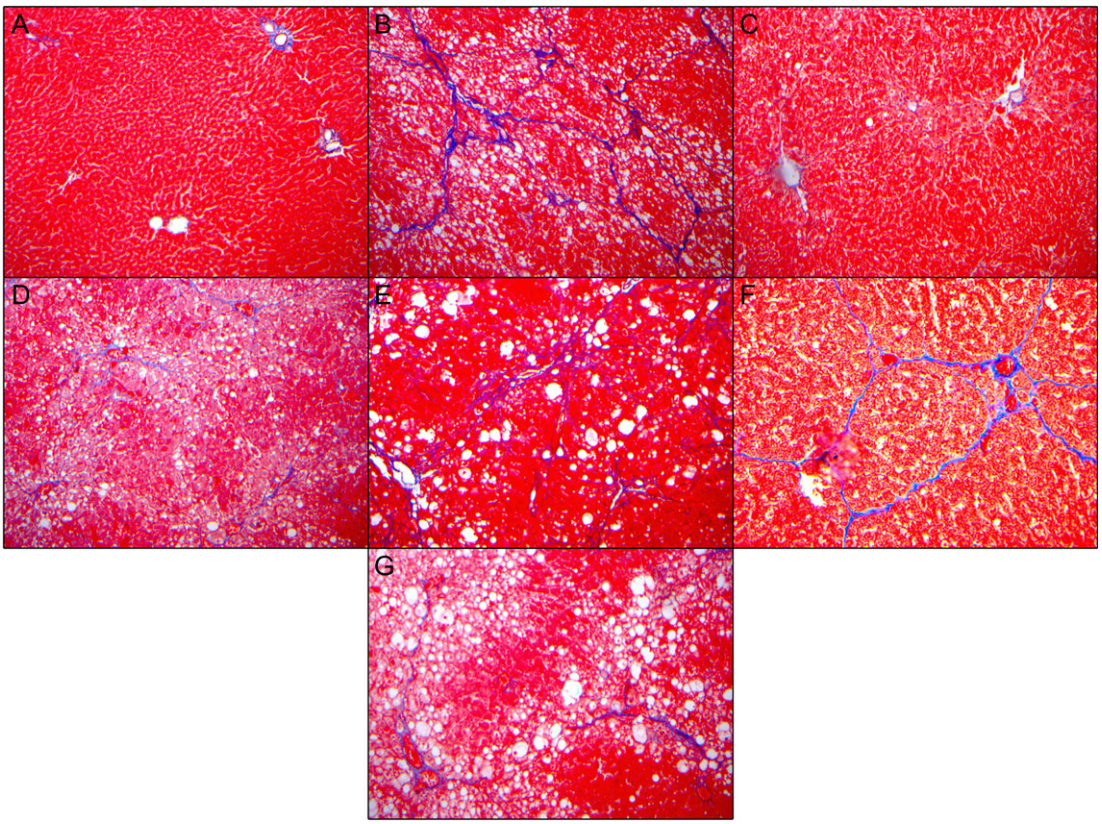

Figure 1. Masson staining analysis (A) Masson staining in the normal group. (B) Masson staining in the model group. (C) Masson staining in the EPA high-dose group. (D) Masson staining in the EPA medium-dose group. (E) Masson staining in the EPA low-dose group. (F) Masson staining in the notoginseng salvia miltiorrhiza group. (G) Masson staining in the colchicine group. Magnification, ×100.

Effect of EPA on histological activity and fibrosis stages

As shown in **Table 3**, rank sum test indicated statistically significant difference in the histological activity and fibrosis stages between all treatment groups and the model group ($P < 0.01$). Unfortunately, none of the EPA groups were significantly different from the notoginseng salvia miltiorrhiza and colchicine groups in either of these parameters ($P > 0.05$).

Effect of EPA on the expressions and distributions of NF-κB, α-SMA, TGF-β1, and TIMP-1 in liver tissues

To further elucidate the molecular mechanism involved in the anti-fibrotic effects of EPA and the roles of NF-κB, α-SMA, TGF-β1, and TIMP-1 in hepatic fibrosis, the expression levels of NF-κB, α-SMA, TGF-β1, and TIMP-1 in liver tissues were examined by immunohistochemistry (**Figs. 3–6**). Under physiological conditions, NF-κB, α-SMA, TGF-β1, and TIMP-1 are expressed in moderate levels in hepatocytes. However, the expression levels of NF-κB, α-SMA, TGF-β1, and TIMP-1 were markedly higher in the model group than those in the normal group ($P < 0.01$). NF-κB is mainly expressed and distributed in the nucleus and partly in the cytoplasm, whereas α-SMA is predominantly expressed in the cytoplasm of hepatocytes. The expression and distribution of TGF-β1 in portal vein, portal tracts, and hepatocyte cytoplasm around the portal area was significantly increased. TIMP-1 was stained brownish yellow. The positive expression of the TIMP-1 protein was primarily observed in hepatocyte cytoplasm in the model group, and the expression and distribution of TIMP-1 was increased with the extent of liver fibrosis. Moreover, as shown in **Table 4**, compared with that in the model group, the expressions of NF-κB, α-SMA, TGF-β1, and TIMP-1 were markedly attenuated in the EPA, notoginseng salvia miltiorrhiza, and colchicine groups ($P < 0.05$ for all).

Discussion

Hepatic fibrosis has been widely accepted as a wound-healing response of the liver against a variety of stimuli, including viral hepatitis, drug exposure, and the presence immune compounds or copper deposition. Hepatic fibrosis is a chronic liver condition that is characterized by the excessive deposition of extracellular matrix (ECM) components around the sinusoidal layer and the distortion of liver tissue architecture [8,9].

The ECM is degraded by matrix metalloproteinases (MMPs) and TIMP-1 is an antagonist of MMPs [10]. Moreover, the activation and the proliferation of hepatic stellate cells (HSCs) have been considered a key event for ECM accumulation and excessive collagen deposition during hepatic fibrosis. Increasing the activation of MMPs, inhibiting the expression of TIMP-1, and suppressing the activation of HSCs have emerged as important treatment strategies for hepatic fibrosis [11].

CCl_4-induced hepatic injury is a well-established model for the study of hepatic fibrosis. EPA is a traditional Chinese medicinal compound that is obtained from *P. americana* using modern isolation technologies. In this study, we demonstrated the effects of EPA

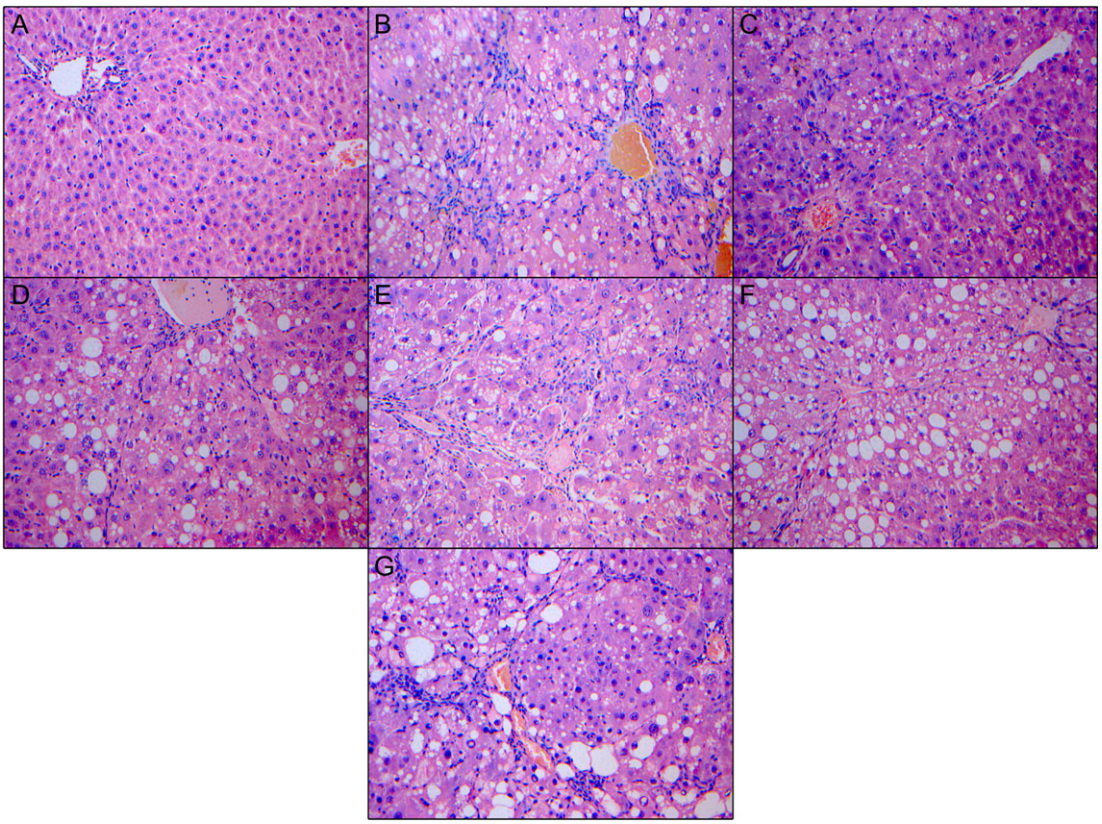

Figure 2. H&E staining analysis (A) H&E staining in the normal group. (B) H&E staining in the model group. (C) H&E staining in the EPA high-dose group. (D) H&E staining in the EPA medium-dose group. (E) H&E staining in the EPA low-dose group. (F) H&E staining in the notoginseng salvia miltiorrhiza group. (G) H&E staining in the colchicine group. Magnification, ×200.

Table 3. Comparison of histological activity and fibrosis stages

Groups	*n*	A					F				
		A0	A1	A2	A3	A4	F0	F1	F2	F3	F4
Normal	10	9	1	0	0	0	10	0	0	0	0
Model	9	0	0	2	5	2^a	0	0	0	2	7^a
EPA high dose	9	0	3	5	1	0^b	0	2	6	1	0^b
EPA medium dose	10	0	3	4	3	0^b	0	3	5	2	0^b
EPA low dose	10	0	2	5	3	0^b	0	2	2	6	0^b
Drug 1	10	0	1	4	5	0^b	0	1	3	5	1^b
Drug 2	10	0	2	4	4	0^b	0	1	3	5	1^b

A, histological activity, A0–A4; F, fibrosis stage, F0–F4.

EPA, extracts of *P. americana*; Drug 1, notoginseng salvia miltiorrhiza; Drug 2, colchicine.

$^aP < 0.01$ compared with the normal group; and $^bP < 0.05$ compared with the model group.

on the prevention and treatment of hepatic fibrosis in a CCl_4-induced hepatic fibrosis model in rats. We determined the anti-fibrotic efficacy of EPA and explored the mechanisms of EPA action in various CCl_4-induced hepatic fibrosis models via the evaluation of relevant cytokines.

It was found that EPA treatment significantly decreased the serum levels of ALT and AST, and increased the serum levels of Alb, HA, LN, PC III, and IV-C, which are important indices reflecting the degree of hepatic fibrosis. The serum levels of HA, LN, PC III, and IV-C were much higher in the model group than those in the normal group, and the levels of HA, LN, PC III, and IV-C were much lower in the EPA groups than those in the model, notoginseng salvia miltiorrhiza, and colchicine groups. As shown in **Tables 1** and **2**, EPA could improve liver function in rats with CCl_4-induced liver damage and attenuate CCl_4-induced hepatic fibrosis. In addition, histopathological examination demonstrated a markedly high number of inflammatory cell infiltrates, significant adipose degeneration of hepatocytes, extensive necrosis of hepatocytes around the lobule, and increased deposition of collagen fibers in hepatic lobules in CCl_4-treated rats compared with those in untreated rats. However, EPA treatment reduced the above histological changes relative to those in the model group treated with CCl_4.

TGF-β1 is known as one of the strongest promoters of hepatic fibrosis, and it causes HSCs to secrete more TGF-β1 through an autocrine loop, also known as the positive feedback mechanism, thereby inducing HSCs to synthesize collagen. TGF-β1 plays a key role in the progression of hepatic fibrosis by affecting cell development, HSC activation, collagen deposition and ECM remodeling [12]. TIMPs are the most important enzymes that regulate the activity of extracellular MMPs. One such enzyme is TIMP-1 that is mainly secreted by activated HSCs and induced by a variety of cytokines. With the development of hepatic fibrosis, the level of TIMP-1 progressively increases; however, its activity gradually decreases, and the degradation of ECM components including type I and III collagens is inhibited, resulting in the excessive deposition of ECM and acceleration of hepatic fibrosis [13]. Our results showed that the

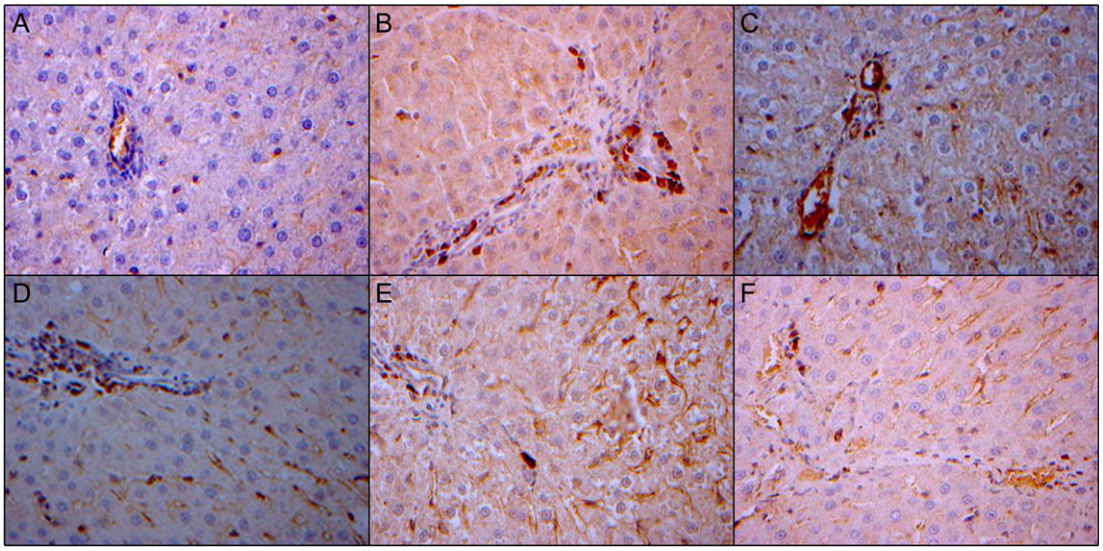

Figure 3. The expression level of NF-κB determined by immunohistochemistry (A) Normal group NF-κB. (B) Model group NF-κB. (C) EPA high-dose group NF-κB. (D) EPA medium-dose group NF-κB. (E) EPA low-dose group NF-κB. (F) Notoginseng salvia miltiorrhiza group NF-κB. It shows that NF-κB is mainly expressed and distributed in the nucleus and partly in the cytoplasm. Magnification, ×400.

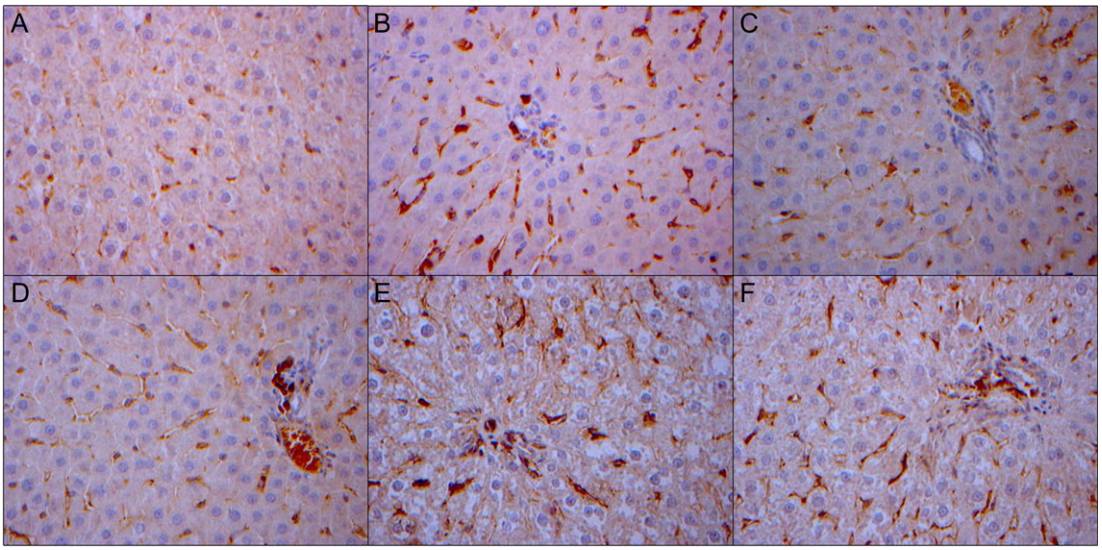

Figure 4. The expression level of α-SMA determined by immunohistochemistry (A) Normal group α-SMA group. (B) Model group α-SMA. (C) EPA high-dose group α-SMA. (D) EPA medium-dose group α-SMA. (E) EPA low-dose group α-SMA. (F) Notoginseng salvia miltiorrhiza group α-SMA. α-SMA is predominantly expressed in the cytoplasm of hepatocytes. Magnification, ×400.

expression levels of TGF-β1 and TIMP-1 were markedly higher in the model group than those in the normal group, while EPA clearly reduced these levels. The high expressions of TGF-β1 and TIMP-1 in the model group are consistent with the positive feedback mechanism between HSC activation and TGF-β1 secretion, indicating that this mechanism promotes the formation and development of CCl_4-induced hepatic fibrosis. The continuous activation of HSCs results in the secretion of high levels of TIMP-1, which further aggravates hepatic fibrosis. However, little is known regarding whether EPA alleviates CCl_4-induced hepatic fibrosis by inhibiting the expressions of TGF-β1 and TIMP-1.

α-SMA has been regarded as a marker of HSC activation. Under quiescent conditions, HSCs do not express α-SMA. But in response to inflammatory mediators and cytokines, HSCs are activated, and they express α-SMA, rapidly proliferate and synthesize substantial amounts of ECM components. Therefore, during the process of liver fibrogenesis, activated HSCs, characterized by the high expression of α-SMA, are the primary sources of ECM. NF-κB, a nuclear transcription factor that is widely present in cells, regulates the expressions of numerous cytokines and inflammatory mediators, and participates in immune responses, signal transduction and other important cellular functions [14].

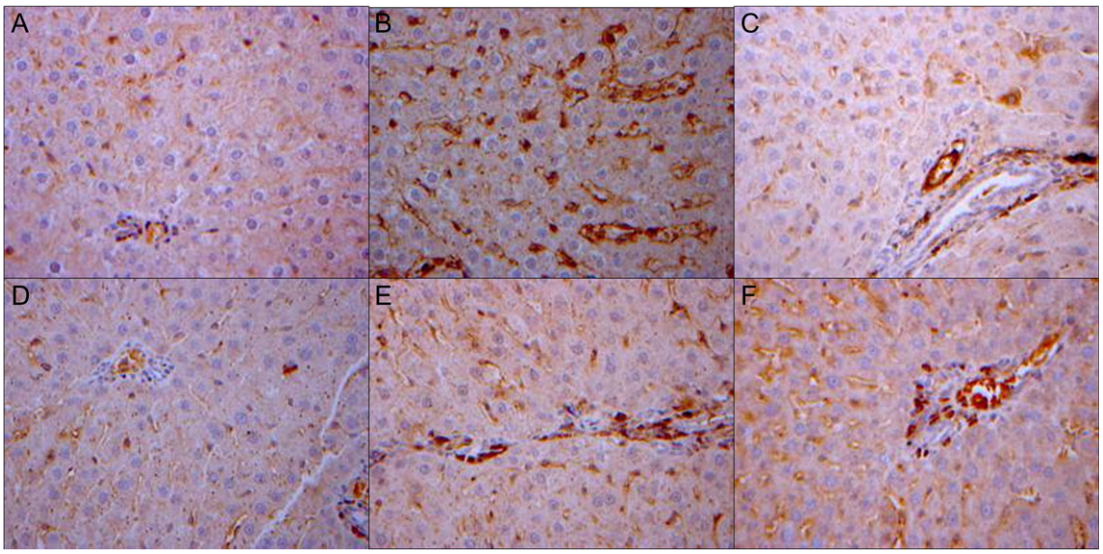

Figure 5. The expression level of TGF-β1 determined by immunohistochemistry (A) Normal group TGF-β1. (B) Model group TGF-β1. (C) EPA high-dose group TGF-β1. (D) EPA medium-dose group TGF-β1. (E) EPA low-dose group TGF-β1. (F) Colchicine group TGF-β1. The expression and distribution of TGF-β1 in portal vein, portal tracts, and hepatocyte cytoplasm around the portal area was significantly clear. Magnification, ×400.

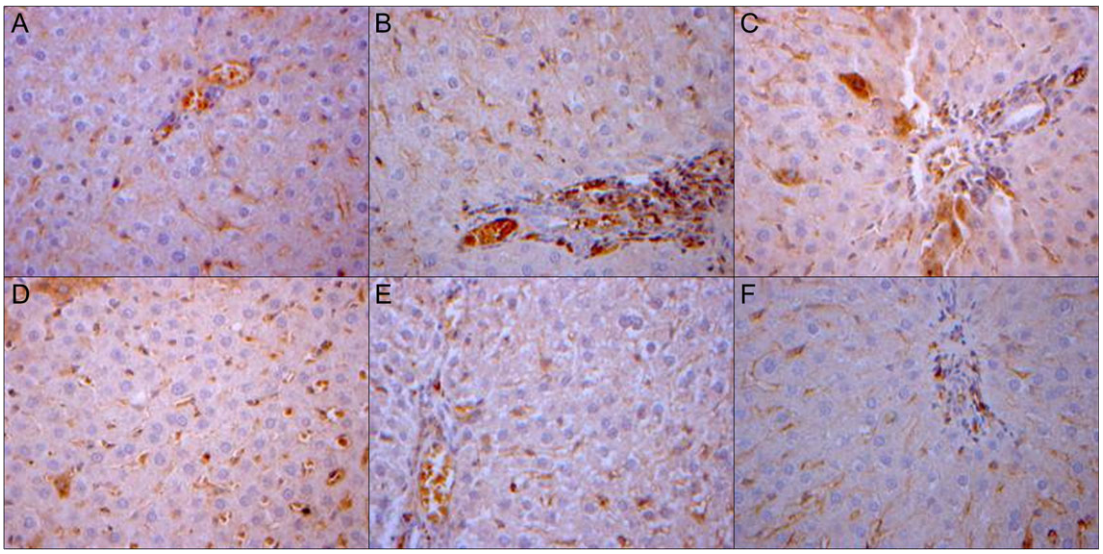

Figure 6. The expression level of TIMP-1 determined by immunohistochemistry (A) Normal group TIMP-1. (B) Model group TIMP-1. (C) EPA high-dose group TIMP-1. (D) EPA medium-dose group TIMP-1. (E) EPA low-dose group TIMP-1. (F) Colchicine group TIMP-1. The positive expression of the TIMP-1 protein was primarily observed in hepatocyte cytoplasm in the model group. Magnification, ×400.

Under normal circumstances, the trimeric complex composed of NF-κB and its inhibitory factor IκB remains sequestered in the cytoplasm and does not participate in nuclear transcription. After dissociation from IκB, NF-κB is activated, and translocated into the nucleus, where it regulates the transcription of genes encoding various inflammatory molecules [15]. A previous study has indicated that activation of NF-κB can also activate the expression of the downstream gene encoding collagen, thus further accelerating the occurrence and development of hepatic fibrosis [16]. Our data showed that there is a greater extent of NF-κB- and α-SMA-positive area in the model group than that in the normal or the EPA group. Furthermore, EPA treatment markedly attenuated the expressions of NF-κB and α-SMA compared with the model group. Thus, the inhibition of HSC activation and reduction in NF-κB expression by EPA likely mediated the effects of EPA on CCl_4-induced hepatic fibrosis.

In conclusion, our data showed that EPA treatment significantly reduced the serum levels of ALT and AST, improved the serum levels of Alb, reduced other hepatic fibrosis-related serum detection indices, protected liver cells from damage, reduced inflammatory cell infiltration, attenuated the synthesis and deposition of collagen fibers, and markedly ameliorated hepatic fibrosis in rats. EPA is effective in the prevention and treatment of hepatic fibrosis, and may be used as a potential therapeutic compound for treating hepatic fibrosis. The mechanism of EPA action may be related to the inhibition of the expressions of TGF-β1, NF-κB, and α-SMA, as well as the reduction of TIMP-1 level in the liver to reduce the accumulation of ECM components,

Table 4. Comparison of immunohistochemical staining area for NF-κB, α-SMA, TGF-β1, and TIMP-1

Groups	*n*	NF-κB	α-SMA	TGF-β1	TIMP-1
Normal	10	13.62 ± 4.96	22.99 ± 1.19	23.99 ± 10.70	19.38 ± 2.52
Model	9	44.90 ± 5.14[a]	63.02 ± 5.37[a]	68.45 ± 11.91[a]	66.77 ± 8.47[a]
EPA high dose	9	18.03 ± 4.76[b]	27.91 ± 6.18[b]	34.68 ± 6.37[b]	32.43 ± 2.02[b]
EPA medium dose	10	20.55 ± 7.39[b]	29.44 ± 5.26[b]	39.94 ± 3.62[b]	35.89 ± 7.45[b]
EPA low dose	10	25.04 ± 5.37[b]	36.62 ± 3.56[b]	48.58 ± 7.95[b]	54.72 ± 6.49[b]
Drug 1	10	27.33 ± 5.17[b]	43.41 ± 4.34[b]	48.39 ± 10.34[b]	55.23 ± 6.50[b]
Drug 2	10	30.90 ± 5.36[b]	45.79 ± 3.88[b]	47.82 ± 8.16[b]	55.89 ± 7.23[b]

Data are presented as the mean ± SD.
EPA, extracts of *P. americana*; Drug 1, notoginseng salvia miltiorrhiza; Drug 2, colchicine.
[a]$P < 0.01$ compared with the normal group; and [b]$P < 0.05$ compared with the model group.

thereby blocking the relevant signaling pathways and preventing the inflammatory responses to attenuate or reverse hepatic fibrosis. Nevertheless, hepatic fibrosis is a very complicated process, and the effects of EPA and the associated molecular mechanisms in the attenuation or reversal of hepatic fibrosis need to be further explored.

Funding

This work was supported by the grants from the Natural Foundation Surface Project of Yunnan Province (No. 2009CD087) and Yunnan Provincial Science and Technology Department—Kunming Medical University Joint Fund Key Project [No. 2017FE468(-173)].

References

1. Zhang Y, Li XM, Zhang FK, Wang BE. Activation of canonical Wnt signaling pathway promotes proliferation and self-renewal of rat hepatic oval cell line WB-F344 *in vitro*. *World J Gastroenterol* 2008, 14: 6673–6680.
2. Dongiovanni P, Remeo S, Valenti L. Hepatocellular carcinoma in nonalcoholic fatty liver:role of environmental and genetic factors. *World J Gastroenterol* 2014, 20: 12945–12955.
3. Friedman SL, Rockey DC, Bissell DM. Hepatic fibrosis 2006: report of the third AASLD single topic conference. *Hepatology* 2007, 45: 242–429.
4. Ma JH, Jiang QM, Xu H, Zhang YY, Zeng M, Yang M. Anti-liver injury and mechanism of *Periplaneta americana* on CCl4-induced liver injury. *Chin J Pharmacol Clin* 2008, 24: 79–80.
5. Du YM, Chen HS, Li SN, Li Z, Li XB, Zhang HM, Fang CS. Preliminary study on pharmacodynamics of GanLong capsule in treating hepatitis B virus. *Lishizhen Med Mater Med Res* 2006, 17: 1369–1371.
6. Li W, Duan LF, He GQ, Shen ZQ, Yang HQ, Liang YP. Effects of *Periplaneta americana* extraction on experimental hepatic fibrosis. *Lishizhen Med Mater Med Res* 2010, 21: 1137–1138.
7. Li W, Duan LF, He GQ, Liang YP, Zhang YF, Yang HQ, Shen ZQ, *et al*. Effects of different doses of *Periplaneta americana* extraction on hepatic fibrosis in rats. Chinese. *J Hepatol* 2009, 17: 948–950.
8. Ding J, Yu JP, Wang CD, Hu W, Li D, Luo YJ, Luo HS, *et al*. Ginkgo biloba extract alleviates liver fibrosis induced by CCl_4 in rats. *Liver Int* 2005, 25: 1224–1232.
9. Gao B, Bataller R. Alcohnic liver disease: pathogenesis and new therapeutic targets. *Gastroenterology* 2011, 141: 1572–1585.
10. Wu LM, Wu XX, Sun Y, Kong XW, Zhang YH, Xu Q. A novel synthetic oleanolic acid derivative (CPU-II2) attenuates liver fibrosis in mice through regulating the function of hepatic stellate cells. *Biomed Sci* 2008, 5: 251–259.
11. Woodhoo A, Iruarrizaga-Lejarreta M, Beraza N, García-Rodríguez JL, Embade N, Fernández-Ramos D, Martínez-López N, *et al*. Human antigen R contributes to hepatic stellate cell activation and liver fibrosis. *Hepatology* 2012, 56: 1870–1882.
12. Roderburg C, Luedde M, Vargas Cardenas D, Vucur M, Mollnow T, Zimmermann HW, Koch A, *et al*. miR-133a mediates TGF-β-dependent derepression of collagen synthesis in hepatic stellate cells during liver fibrosis. *J Hepatol* 2013, 58: 736–742.
13. Fowell AJ, Collins JE, Duncombe DR, Pickering JA, Rosenberg WMC, Benyon RC. Silencing tissue inhibitors of metalloproteinases (TIMPs) with short interfering RNA reveals a role for TIMP-1 in hepatic stellate cell proliferation. *Biochem Biophys Res Commun* 2011, 407: 277–282.
14. Mann D, Smart D. Transcriptional regulation of hepatic stellate cell activation. *Gut* 2002, 50: 891–896.
15. Wu J, Zern MA. NF-kappa B, liposomes and pathogenesis of hepatic injury and fibrosis. *Front Biosci* 1999, 4: D520–D527.
16. Elsharkawy AM, Mann DA. Nuclear factor-κB and the hepatic inflammation fibrosis cancer axis. *Hepatology* 2007, 46: 590–597.